

Relating Urban Morphology and Urban Heat Island During Extreme Heat Events in the Kansas City Metropolitan Area

By
© 2018

Rodney M. Chai
B.A., Haverford College, 2015

Submitted to the graduate degree program in Atmospheric Science and the Graduate Faculty of the University of Kansas in partial fulfillment of the requirements for the degree of Master of Science.

Chair: Dr. Nathaniel A. Brunsell

Dr. David A. Rahn

Dr. Ward Lyles

Date Defended: 19 April 2018

The thesis committee for Rodney M. Chai certifies that this is the approved version of the following thesis:

Relating Urban Morphology and Urban Heat Island During Extreme Heat Events in the Kansas City Metropolitan Area

Chair: Dr. Nathaniel A. Brunsell

Date Approved: 19 April 2018

Abstract

Satellite images offer continuous spatial and temporal coverage of surface temperature, thus allowing us to transcend limitations of in-situ measurements and giving us a powerful tool to understand the Urban Heat Island (UHI). This study uses MODIS Land Surface Temperature (LST) at 1 km to examine the relationship between urban morphology and UHI. Using the Kansas City metropolitan area as a case study, we examined MODIS LST data during the summer months of 2002-2017. We found that LST anomalies increase exponentially from 1.5°C at the 90-95 percentile to 3.5°C at the 95-100 percentile. In particular, natural land cover LCZ classes are found to have higher LST anomalies than built-type LCZ classes by up to 5°C. Results suggest that the higher LST anomalies over outlying areas are not due to suburban development during the most extreme heat episodes. We also examined the utility of the LCZ scheme during extreme heat events. We found that the LST response is not statistically different between the various LCZ classes and that the local built environment is not as important in predicting the LST response to increasingly extreme heat events. However, the LST response by most LCZ classes as a function of distance from downtown is statistically significant, with values ranging from -0.08°C/km to -0.01°C/km. The results show that the distance from the city center plays a more important role in helping predict LST response than knowledge of the LCZ class.

Acknowledgements

I would like to thank my advisor, Dr. Nathaniel Brunsell, for the countless hours of discussion and guidance. I would also like to thank Dr. David Rahn and Dr. Ward Lyles for serving on my committee and providing helpful feedback during my proposal defense. I also want to extend my deep gratitude towards Dr. David Mechem and Brian Barjenbruch, a meteorologist currently with NWS Omaha/Valley for encouraging me to make the switch from MS Geography to MS Atmospheric Science so I can formally pursue my passion in weather. It was certainly a huge leap of faith to switch from philosophy to a hard science but I have been thoroughly thrilled to pursue my dream!

I also want to thank the undergraduate Atmospheric Science majors from the Class of 2018. I remember the days when we worked on problem sets for Dynamic Meteorology and Physical Meteorology at the MACH during my initial switch to meteorology. I also want to thank all the faculty and graduate students in the Department of Geography and Atmospheric Science whom I have had the pleasure of meeting during my time at KU. I also want to thank all the ATMO 105 undergraduate students whom I had the honor of teaching. Your curiosity and motivation to learn about weather made my teaching duties so much more enjoyable. Also a special thanks to Dr. Justin Stachnik for being such a passionate ATMO 105 lecturer and supervisor of the lab TAs. I also want to give a special shout out to Brandon Burton, one of my former ATMO 105 students for introducing me to (severe) storm chasing. I also cannot forget the staff in the Lindley Welcome Center who has made my time at KU more pleasant.

Looking back, I want to thank the professors at my alma mater Haverford College who have taught me how to think and write well. Haverford was also the place I fell in love with

snow. And last but not least, a big thank you to my parents and sister for supporting me on my graduate school career and always being there for me.

Table of contents	v
1 Introduction	1
2 Methodology	5
2.1. Overview of the study area.....	5
2.2. Identification of heat wave days.....	7
3 Results	9
3.1. Comparing LST anomalies across LCZ classes for extreme heat events.....	9
3.2. Spatial distribution of LST.....	13
3.3. LCZ as a function of distance from downtown.....	19
4 Discussion and conclusion	26
References	30

CHAPTER 1

Introduction

With rapid urbanization in the past few decades, over half of the world population now live in urban areas for the first time in history (WHO 2010). The phenomenon where the urban center is warmer than the surrounding rural areas is known as the Urban Heat Island (UHI), which can be primarily attributed to the greater thermal capacity of the material used to build roads and high-rises, such as asphalt and concrete (Oke 1982). The high fraction of impervious surfaces in cities modifies the surface energy balance and weather processes (Roth 2013; Wood et al. 2013). Indeed, several studies have proposed that local land cover composition is a primary determinant of land surface temperature (LST) patterns (Hu et al. 2014; Hu and Brunsell 2013; Li et al. 2013; Connors et al. 2013; Zhou and Wang 2011; Tomlinson et al. 2011). UHI is tied to urban canyons, i.e. urban streets flanked by buildings on both sides (Vardoulakis and et al. 2003). The orientation and height/width ratio affects air circulation and therefore the dissipation of heat (Oke 1988). For example, brick houses, top floor apartments with no through ventilation and closed windows are associated with an increased risk of mortality during a heat wave (Kovats and Hajat 2007). Neighborhoods with greater UHI often have a higher concentration of marginalized groups such as the poor, minorities and elderly relative to less susceptible areas (Bryant-Stephens 2009; Smargiassi et al. 2009). Unsurprisingly, these neighborhoods have reported higher emergency hospital admissions (Kovats and Hajat 2007; Graham and et al. 2016) and mortalities (Peng et al. 2011). It is therefore of critical importance to develop a systematic and reliable way to relate urban morphology and UHI.

Excessive heat events (more commonly known as heat waves), which UHI can potentially exacerbate, are the number one cause of weather-related deaths in the United States

(Roth 2013). According to Robinson (2001), heat waves occur when conditions exceed both the daytime high and the nighttime low thresholds of the same percentile for two consecutive days. Heat waves generally result from stagnant synoptic high pressure systems that are associated with clearer skies, calmer winds and drier soils, which all contribute to higher UHI intensity (Schatz and Kucharik 2015; Loikith and Broccoli 2012; Oke 1982). Between 1999 and 2009, an annual average of 658 heat-related deaths were reported in the United States (Fowler et al. 2013). Anthropogenic climate change also has the capacity to increase the magnitude of the UHI by up to 30 percent (McCarthy et al. 2010). Indeed, global climate models are predicting more frequent, intense, and longer heat waves (Forzieri et al. 2016; Lemordant et al. 2016; Trenberth et al. 2015; Russo et al. 2014; Peng et al. 2011; Fischer and Schar 2010; Meehl and Tebaldi, 2004). Oleson et al. (2011) finds that anthropogenic heat flux from space heating and air conditioning processes contributes about 0.01 W m^{-2} of heat distributed globally. In particular, regions of fast-growing population overlap with areas of high UHI potential (McCarthy et al. 2010).

Until recently, there has been no standardized way to characterize urban morphology (Bechtel et al. 2015). UHI studies have been complicated by the traditional urban-rural distinction, which is subjective and does not always reflect the heterogeneity in land cover in and around a city (Stewart and Oke 2009; Hu and Brunsell 2015). UHI intensity is traditionally defined as the temperature difference between a city and its rural surroundings (Schatz and Kucharik 2015; Stewart and Oke 2012). However, the degree of urban development and thereby the magnitude of UHIs varies continuously across landscapes. Zhou et al. (2017) found that UHI increases with the logarithm of city size and fractal dimension (compactness of a city) but is reduced with the logarithm of anisometry (measure of city shape). To address the shortcoming of

the highly subjective urban-rural distinction, the concept of surface UHI (SUHI) is conceptualized to exclude any rural comparison and allow intra-city comparison based on surface temperature. Instead, it is defined with respect to a spatial reference and ambient (or prevalent) meteorological conditions (Martin et al. 2015). Stewart and Oke (2012) created the Local Climate Zone (LCZ) system, which standardizes urban and rural land cover across a city based on land cover, building structure, material and human activity. The appropriate LCZ is assigned based on surface properties such as vegetative fraction, impervious fraction and albedo as well as building properties like sky view factor and mean building height (Ching et al. 2018; Oke 2006; Unger 2004).

One of the key advantages of the LCZ system is that it provides a culturally neutral platform to classify and compare cities in terms of urban form and urban function (Gal et al., 2015; Stewart and Oke 2012). Each of the 17 LCZ classes is associated with a defined set of value ranges for a set of key urban canopy parameters. These include vegetative fraction, impervious fraction, albedo as well as building properties such as sky view factor, mean building height and the building surface fraction (Oke 2006; Unger 2004). The lowest level of detail (L0) data is used to map cities and their surrounding natural landscape into LCZ classes (Stewart and Oke 2012). Urban experts have used the Landsat-derived L0 data to classify over 80 cities worldwide (Ching et al. 2018; Bechtel and et al. (2017a, 2017b, 2015); Bechtel and Daneke 2012).

The complex nature of cities leads to large temperature differences across neighborhoods, even within a short distance (Harlan et al. 2006). Satellite data offer continuous spatial and temporal coverage of temperature and moisture, thus allowing us to potentially overcome limitations of in-situ temperature measurements (Voogt and Oke 2003). Thus, a key advantage of

using remotely sensed LST is that the variability in surface temperatures measured over the extent of the city more closely approximate the actual living conditions of urban residents than air temperature measured at weather stations that are sparsely distributed across a city (Laaidi et al. 2012).

The strong positive relationship between near-surface air temperature and LST is well established (Yang et al. 2017, Mutiibwa et al. 2015, Sohrabinia et al. 2015, Zeng et al. 2015, Zhang et al. 2015, Jang et al. 2014, Prihodko and Goward 1997). Indeed, the remotely sensed SUHI is often used as an indicator of the effect of building energy use and heat stress (Oke et al. 2017). The SUHI is primarily attributed to the radiative and thermal properties of the building material as well as the moistness of the surrounding natural land cover (Oke et al. 2017). Vegetation may enhance cooling in warm urban environments by increasing the effect of shading and potential transpiration rates (Ramamurthy and Bou-Zeid 2017; Jenerette et al. 2016, Tayyebi and Jenerette 2016; Jenerette et al. 2011). Monaghan et al. (2014) shows that increasing the complexity of urban morphology representation in urban environment can improve the accuracy of urban canopy models.

In this paper, we used the Moderate Resolution Imaging Spectroradiometer (MODIS) LST product to examine the spatial distribution of UHI on days of extreme heat events. Specifically, we examined the UHI response for different LCZ classes as heat events increase become more extreme. Given the above review, the following research question and associated hypothesis was proposed: How are urban morphology and UHI magnitude related? We hypothesized that there is a distinctive spatial pattern of UHI magnitude, which is analogous to the spatial distribution of LCZs. We examined the UHI response for different LCZ classes as heat events become more extreme.

CHAPTER 2

Methodology

2.1. Overview of the study area

We chose the Kansas City metropolitan area as our case study, which includes 4 counties in Kansas (Miami, Johnson, Wyandotte and Leavenworth) and 5 counties in Missouri (Cass, Jackson, Platte, Clay and Ray). Kansas City is the 31st largest metro area in the U.S. with 2.1 million people (DATA USA 2017). We chose Kansas City because of its frequent heat wave episodes, which provides the opportunity to study the variability of the UHI during extreme heat events. Summer heat waves in Kansas City generally occur when high pressure moves to the east of Missouri along with an upper level ridge over the area (Chang and Wallace 1987). In addition, Kansas City is located in the Central Great Plains, where an unprecedented drought occurred in 2012 (Cook et al. 2015; Hoerling et al. 2014).

Figure 1a shows a LCZ map for the Kansas City metropolitan area, which is classified using the System for Automated Geoscientific Analyses geographic information system (SAGA-GIS) and Landsat imagery at 30-meter resolution. The method is described in Bechtel et al. (2015). Training areas (TAs) are created to identify areas of the metropolitan area that exemplify the various LCZ classes. This information is then utilized to classify Landsat scenes into LCZ maps using a Random Forest (RF) classifier (Conrad et al. 2015). Figure 1b shows an example of the heterogeneity in land surface temperature (LST) distribution across Kansas City on Jun 27, 2012 in the midst of a prolonged heat wave.

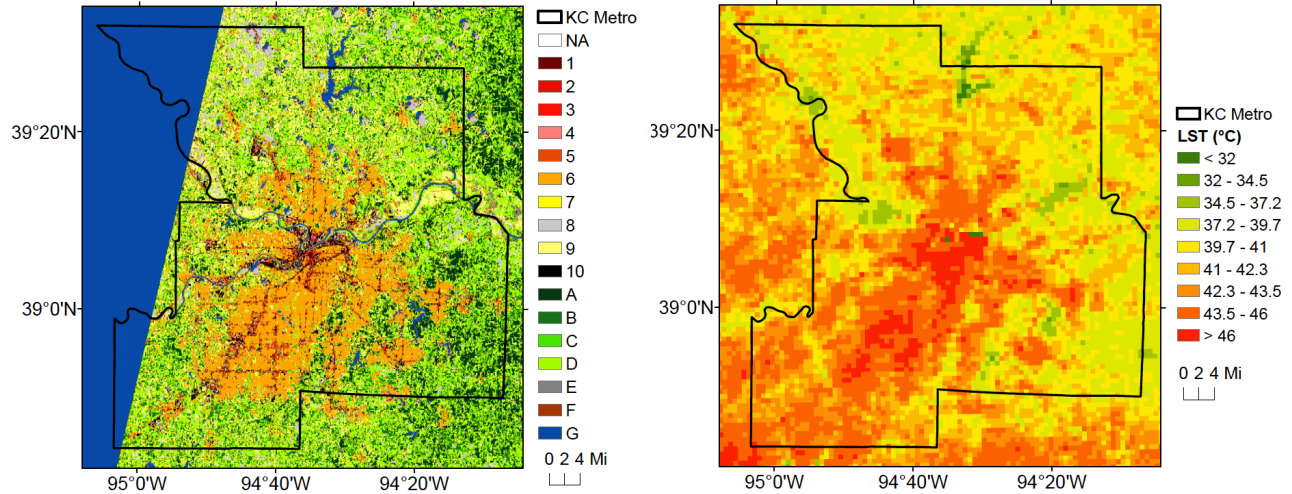


Figure 1. (a) LCZ map of Kansas City metro area. LCZ 1-10 represent urban built-type classes while LCZ A-G are natural cover-type classes (see Table 1). (B) MODIS Land Surface Temperature (LST) image of Kansas City metropolitan area on Jun 27, 2012.

Due to reduced sample size of certain LCZ classes (Table 1), we consolidated similar LCZ classes to conduct spatial analyses. LCZ class 1, 3, 4, 5 and 6 were classified as the dense urban class group. Class 7, 8, 9 and 10 are the sparse urban class group. Finally, LCZ class A, B, D and G are in the natural land cover type group. The LCZ map was resampled using nearest neighbor to match the spatial resolution of MODIS LST product. Because of the scarcity of pixels for LCZ class 1, 3, 4, 7 and E, these classes are not considered during the LST anomaly analysis. In addition, water bodies (LCZ Class G) are not included in the LST anomaly analysis.

Table 1. Pixel breakdown by LCZ class following resampling by nearest neighbor

LCZ	Description	Number of pixels
1	Compact high-rise	9
3	Compact low-rise	2
4	Open high-rise	6
5	Open mid-rise	134
6	Open low-rise	1364
7	Lightweight low-rise	46
8	Large low-rise	494
9	Sparsely built	1065
10	Heavy industry	151

A	Dense trees	1643
B	Scattered trees	460
D	Low plants	5723
E	Bare rock or paved	31
G	Water	3059
NA		164
Total		14351

2.2. Identification of heat wave days

In this paper, we used MODIS LST product at 1km (MYD11_L2) to study LST response based on urban morphology during extreme heat episodes. The key advantage of MODIS products is their daily temporal resolution, which enabled us to examine all heat wave days between 2002-2017 to assess the LST response to increasingly extreme heat events. The metropolitan area is approximately 80km north-south and 80km east-west, and therefore the 1km spatial resolution is deemed sufficient to perform neighborhood analysis and assess the effect of urban morphology on UHI.

We examined all available summer months of MODIS LST data (2002 to 2017). In order to account for potential suburban development and changes in the LCZ class over time, we linearly removed the long-term LST trend in 10 day moving windows between May 1 and Sep 30 for each LCZ class for every pixel. This is particularly pertinent for areas southwest of downtown Kansas City, such as Johnson County, Kansas that have rapidly developed over the past two decades.

Heat wave days are classified by every 5th percentile from 70-100 percentile based on all available MODIS LST data during the summer months of May to September from 2002-2017. The thresholds are set for every LCZ class by 10-day interval, i.e. beginning from May 1-10 and ending Sep 21-30. We identified days where the LST exceeded the 70th percentile and classified those as heat wave days. Then we categorized these heat wave days from 70-100 percentile by 5-

percentile interval to reflect the increasing severity of the heat wave episodes. The LST anomaly is then calculated by taking the difference at every 5-percentile interval.

CHAPTER 3

Results

3.1. Comparing LST anomalies across LCZ classes for extreme heat events

In order to examine how the LST response for different LCZ classes throughout the summer, we separated the LST data for all identified heat wave days into different months to analyze them by their respective LCZ classes. Figure 2 shows the average LST distribution by LCZ class in 10-day windows. The months of May to August are shown to compare the LST response between early (Figure 2a and 2b) and mid-summer (Figure 2c and 2d). The distribution of median LST generally shows what we expected, i.e. that the natural land cover type classes have lower LST than urban built-type classes. And this LST distribution is similar for different stages of the summer season. LCZ 1 (Compact high-rise) has the highest LST and LCZ A (Dense trees) has the lowest LST in each time period due to the cooling effect of vegetation. The less dense built-type LCZ classes show lower LST than their more dense counterparts (e.g. 1 and 10), demonstrating the positive relationship between urban morphology and UHI. In addition, the natural land cover type LCZ classes generally show lower LST than the built-type LCZ classes. The exception is that in the latter part of summer (Figure 2c and 2d), the natural land cover type LCZ classes (e.g. B and D) are warmer than the sparse urban built-type classes (e.g. 8 and 9). However, they are still cooler than the dense urban built-type classes (e.g. 5 and 6) and industrial class (i.e. 10).

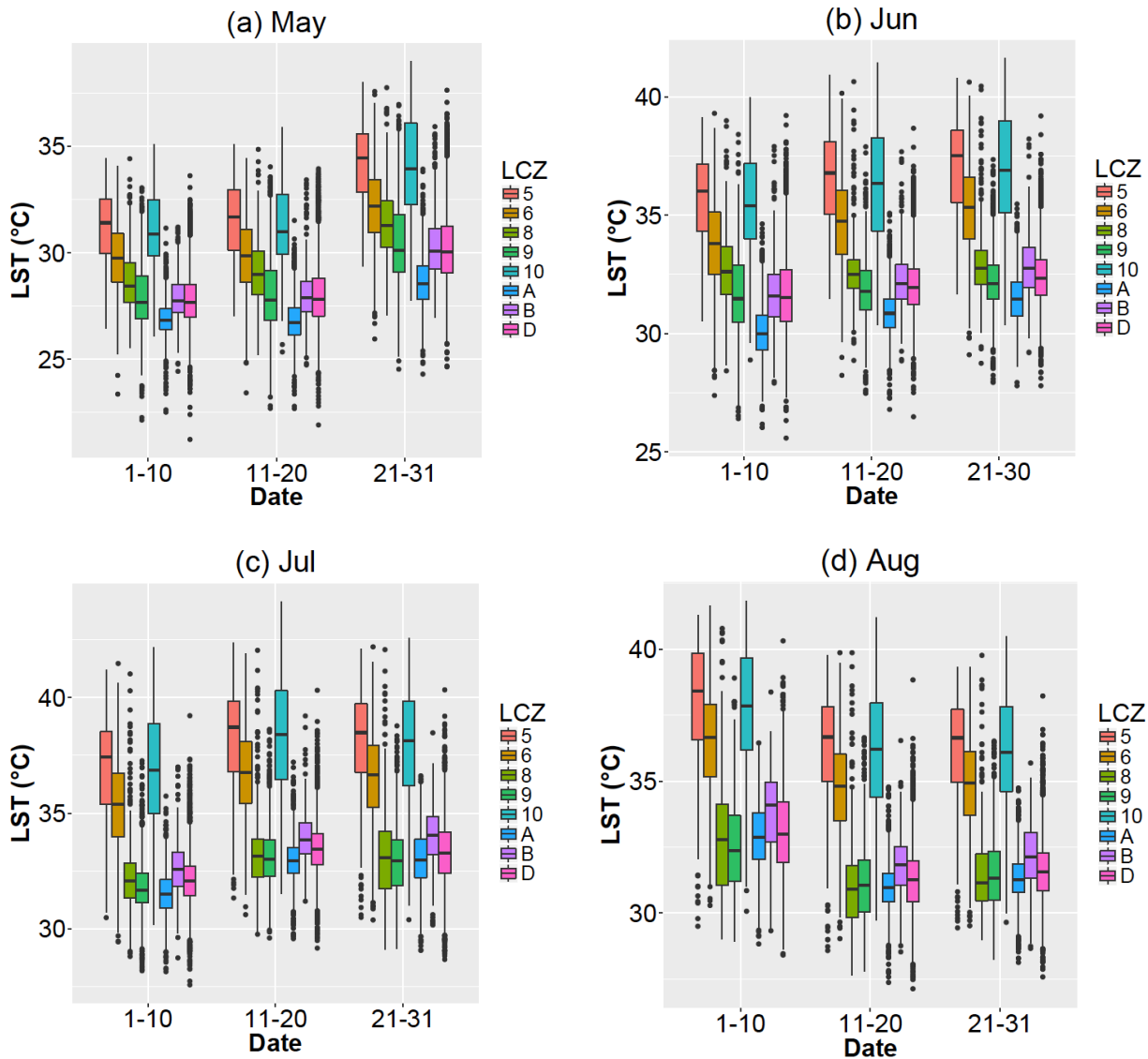


Figure 2. MODIS LST distributions in 10-day intervals by LCZ class

Next, we analyzed the LST anomaly from 70th percentile of all available MODIS LST data to examine the UHI response as heat events become more extreme. With increasing extremity of heat events, the temperature anomaly increases steadily until a sharp jump at the 95-100 percentile for all LCZ classes (Figure 3). For the most predominant built-type LCZ in the Kansas City area (LCZ 6), the average LST increases by 0.57°C between 70-75th percentile. At the 95-100 percentile, the LST anomaly is significantly higher at 3.09°C . It is noteworthy that

the LST response for natural land cover type LCZ classes is higher than that for built-type LCZ classes. This may be somewhat surprising given the cooling effect of vegetation. We will examine possible reasons for the higher UHI response in vegetated areas in subsequent sections.

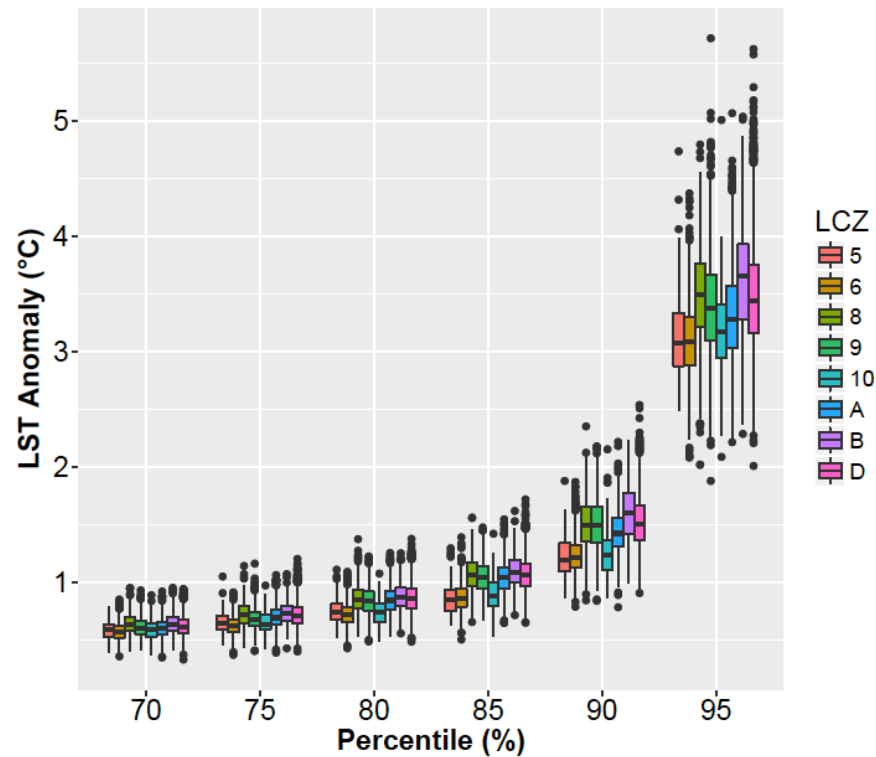


Figure 3. Distributions for selected LCZ classes showing the LST response to increasing heat wave magnitude (70-100 percentile)

In order to compare the individual responses of different LCZ classes to heat wave events, we fit the LST response with an exponential curve in the form of $y=e^{(a+bx)}$ for each LCZ class by every 5th percentile interval and tested for the statistical significance of the regressions. Figure 4 (a-h) shows the exponential relationship between LST anomaly and percentile increase for each LCZ class. The regression of each LCZ class was compared against a general relationship of all LCZ classes (Figure 4i). The LST anomaly regression for each LCZ class is compared to the general regression for all LCZ classes and the results of the two-sample t-test are shown in Table 2. Since the p-values are much larger than 0.05, we concluded that the

difference in the regressions between various LCZ classes and all LCZ classes as a whole is not statistically significant. In other words, knowing the LCZ class does not give us more information about the LST response as a function of increasingly extreme heat events.

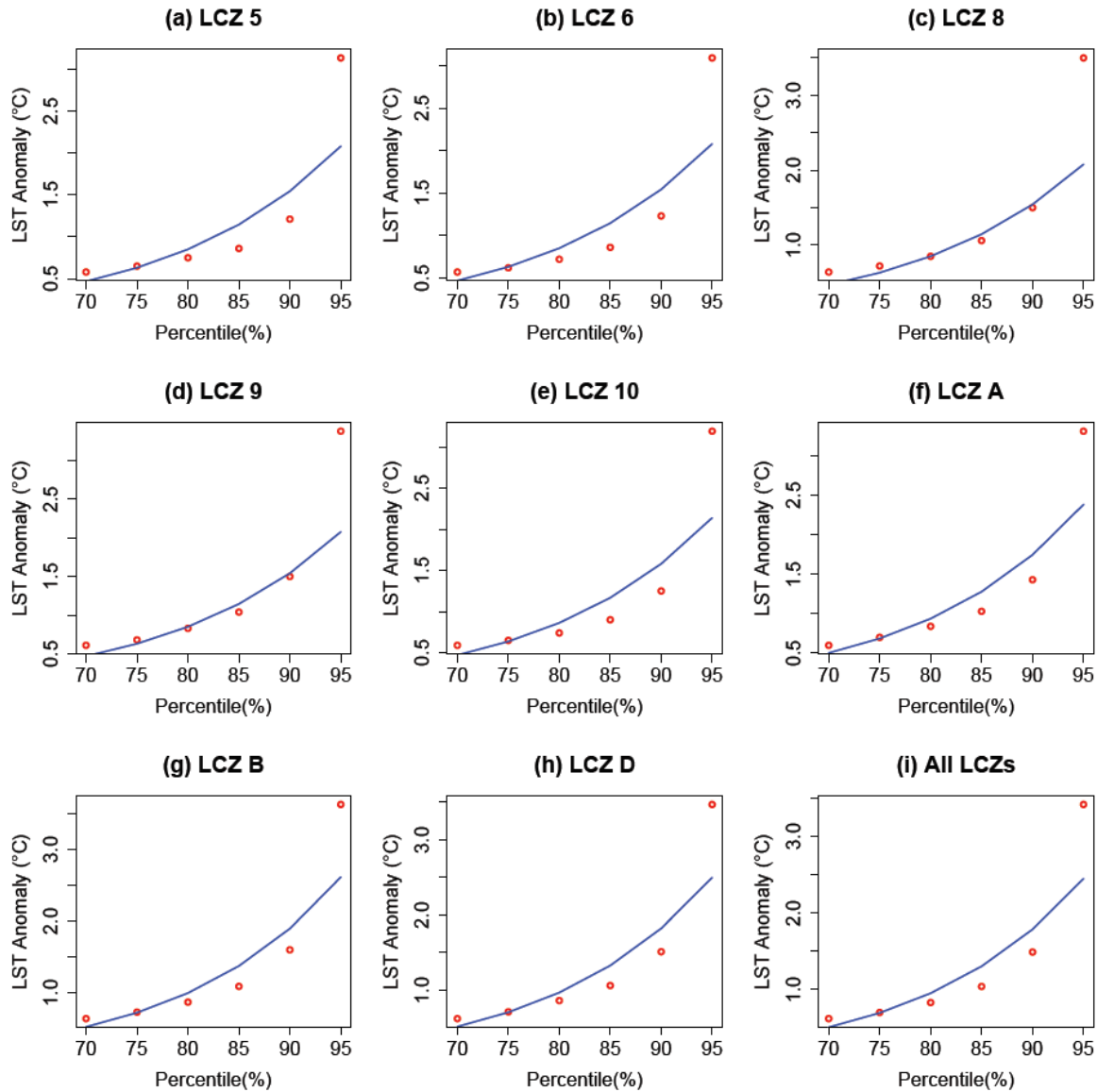


Figure 4. Regressions for LST-anomalies as a function of heat-wave percentile for each LCZ class. The red dots represent the median LST response for every 5th percentile and the blue line is the best-fit exponential curve.

Table 2. Statistical summary for exponential regressions of LST-anomalies as a function of heat-wave percentile (a , b , R^2) and for comparison of various LCZ classes against a general relationship of all LCZ classes using a two-sample t -test (p -value)

LCZ	a	b	R ²	p-value
5	-0.75872	0.0596	0.8073	0.6832
6	-0.79388	0.06105	0.8215	0.6627
8	-0.6499	0.06239	0.8646	0.9541
9	-0.69775	0.06377	0.8818	0.9879
10	-0.7538	0.06055	0.8178	0.7302
A	-0.68717	0.0622	0.8767	0.9503
B	-0.64656	0.06433	0.8792	0.8711
D	-0.66784	0.06334	0.8785	0.9589
All	-0.68011	0.06303	0.872	NA

3.2. Spatial distribution of LST

Since knowing the LCZ class does not give us more information about LST response as heat events become more extreme, we examined the response for different years during the study period. We grouped similar LCZ classes together to facilitate a more effective comparison of LST response to urban morphology: Dense urban built-type (LCZ 5 and 6); sparse urban built-type (LCZ 8 and 9); natural land cover type (LCZ A, B and D) as well as industrial type (LCZ 10). In Figure 5, the years of 2004 and 2012 stand out for having the lowest and highest LST anomalies respectively across all LCZ groups. Based on the number of heat wave days we identified for each summer, the summer of 2012 is the hottest (70 days) and 2004 is the coolest (9 days) during our study period. During the cool summer of 2004, the LST anomaly for natural land cover type group is lower than all other LCZ groups (Figure 5a and 5b). Whereas during the hot summer of 2012, the LST anomaly for the natural land cover type group is higher than those of the other LCZ groups. We then took a closer look at the spatial distribution of LST in those two years.

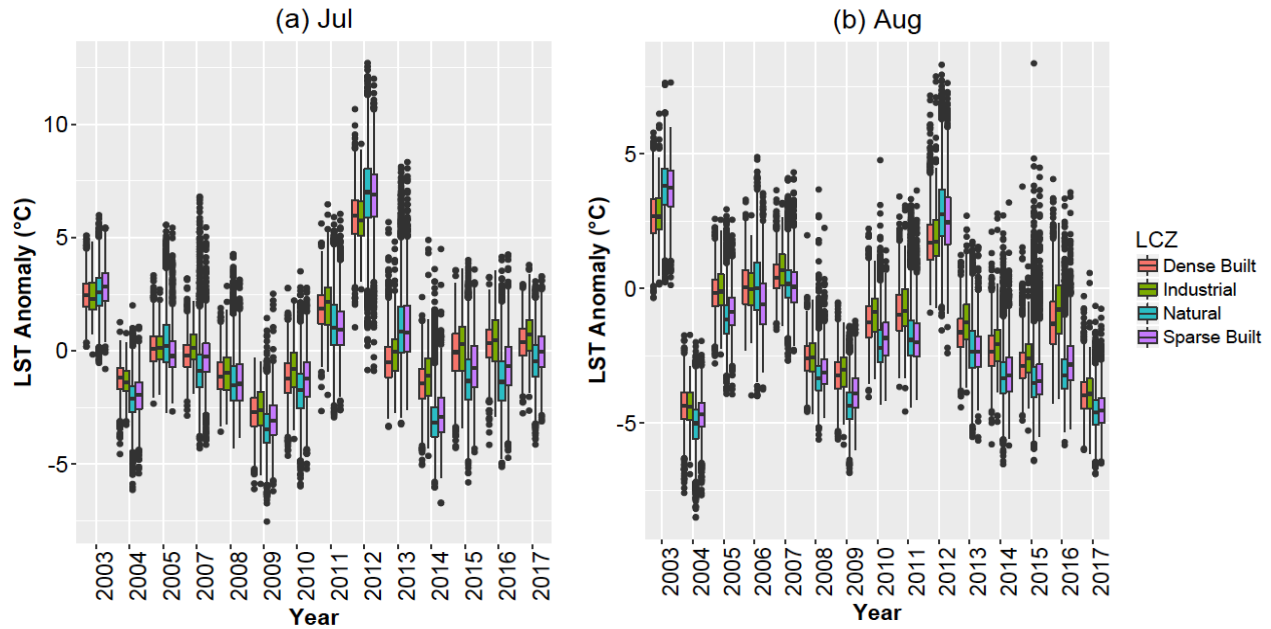


Figure 5. July and August LST anomalies in the Kansas City metropolitan area by year from 2002-2017. The LCZ classes were grouped together according to their similarity: Dense urban built-type (LCZ 1, 3, 4, 5 and 6); Sparse urban built-type (LCZ 7, 8 and 9); Natural land cover type (LCZ A, B and D) as well as Industrial type (LCZ 10).

We examined the mean LST for the Kansas City metropolitan area for the months of July and August in 2004 and 2012 (Figure 6). This coincides with the peak summer heat and the months where most heat wave days occur. As expected, the downtown area is warmer than the surrounding suburbs in both 2004 and 2012 (Figure 6a to 6d). However, there is also a zone of warmer LSTs to the southwest of downtown Kansas City in July and August 2012, which is the year of the anomalously hot summer (Figure 6c and 6d). To better understand the mean LST spatial distribution, we next looked at the spatial distribution of LST anomalies for the same time periods.

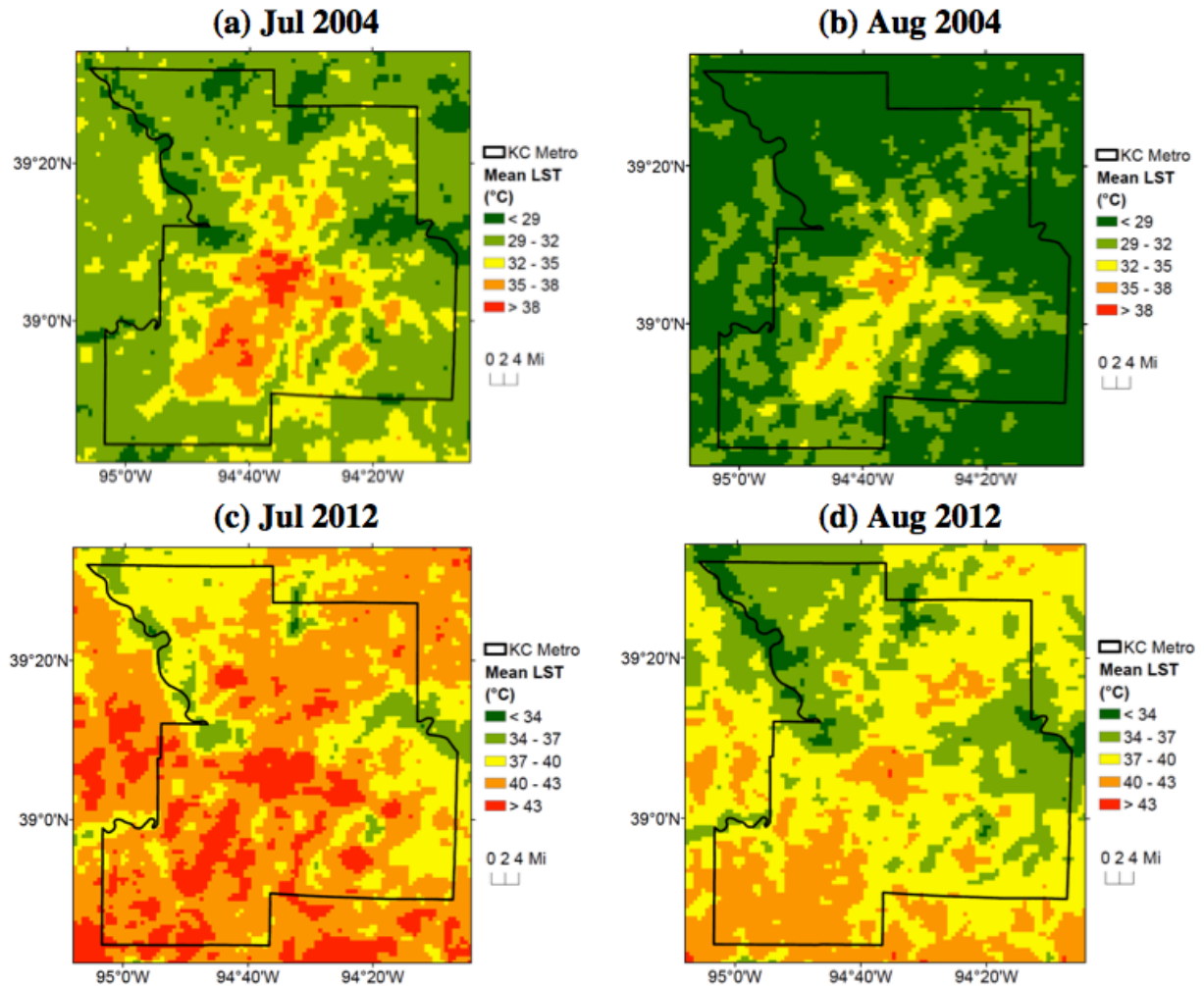


Figure 6. Spatially distributed mean LST for KC metro for the months of July and August in 2004 (cool) and 2012 (hot).

In the cool summer of 2004, LST anomalies are the highest towards downtown and decreases towards the outlying areas (Figure 7a and 7b). In the hot summer of 2012, the pattern is reversed. Outlying areas have higher LST anomalies than downtown (Figure 7c and 7d). So we decomposed all the summers in our study period to the seven warmest and eight coolest summers to see if whether the summer is hot or cool matters for the spatial distribution of LST.

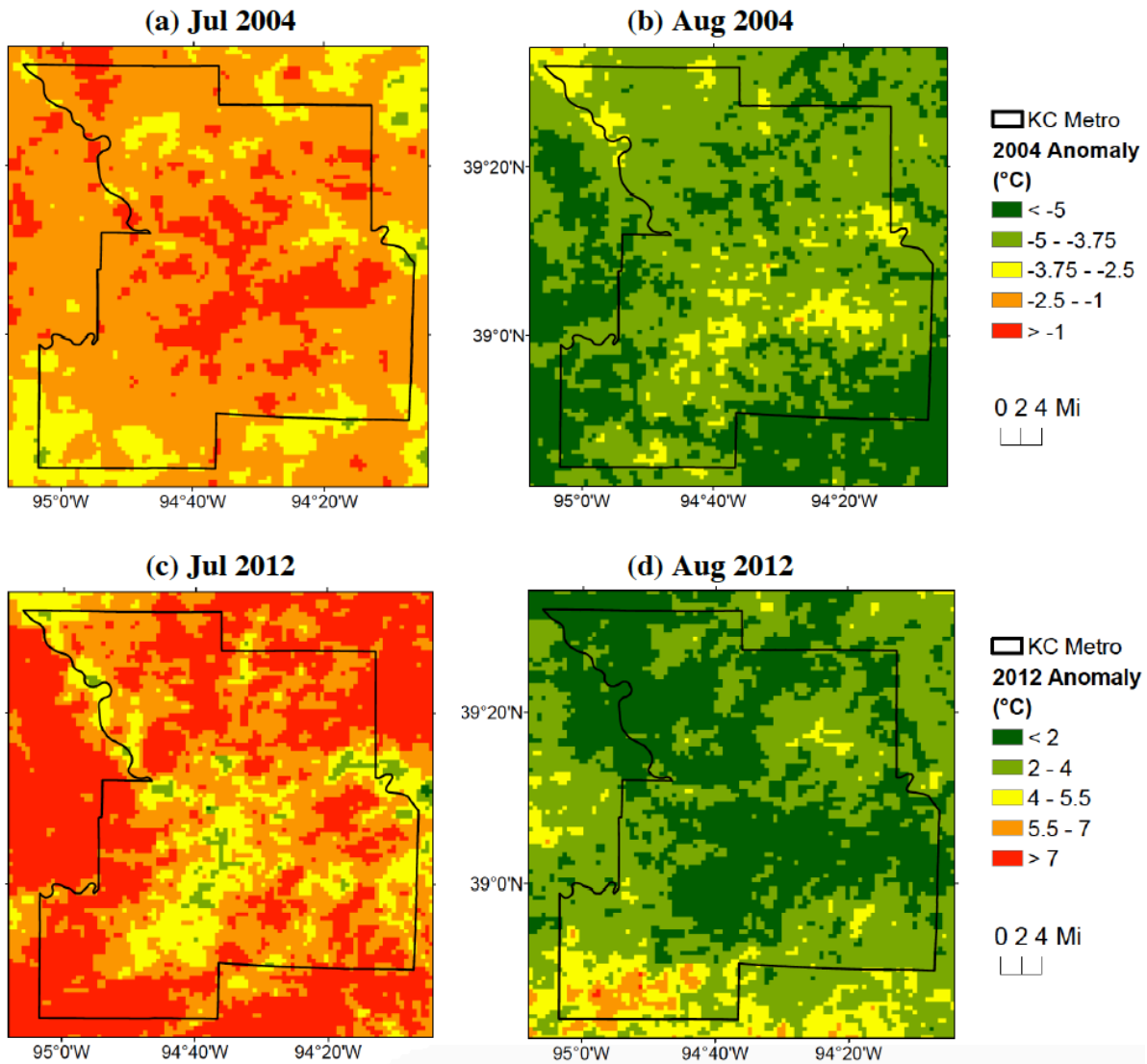


Figure 7. Spatially distributed LST anomalies for KC metro for the months of July and August in 2004 (cool) and 2012 (hot).

As in Figure 5, similar LCZ classes were grouped together to facilitate a more effective comparison of LST response to urban morphology. In general, LST anomaly increases with increasingly extreme heat events. There is a sharp increase in LST anomaly at the 95th percentile for warm summers (Figure 8a) while the increase is more linear for cool summers (Figure 8b).

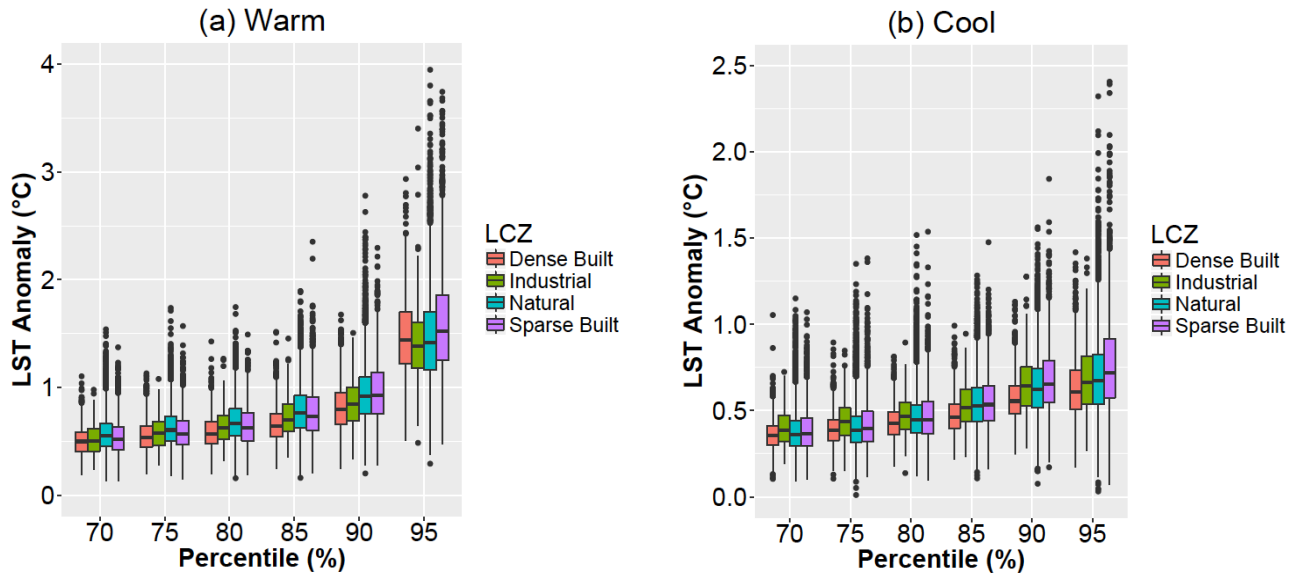


Figure 8. LST anomalies from 70-100th percentile for (a) the 7 warmest summers and (b) the 8 coolest summers during our study period of 2003-2017. As in Figure 5, similar LCZ classes were grouped together to facilitate a more effective comparison of LST response to urban morphology.

We plotted regressions for each of the four LCZ groupings as a function of increasingly extreme heat events (Figure 9 and 10). We then tested for statistical significance in the difference between regression for each LCZ group and for all LCZ classes in general. The results are shown in Table 3a and 3b. While the regressions are found to be significant by themselves, the difference between the regression of the various LCZ groups and that of all LCZ classes is not statistically significant as a function of increasingly extreme heat events.

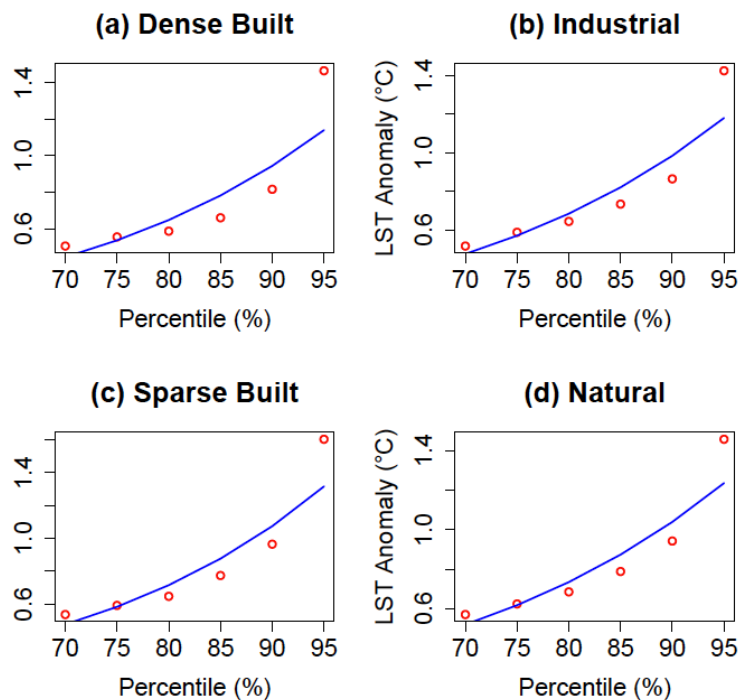


Figure 9. Regressions for LST-anomalies as a function of heat-wave percentile for each LCZ group (Warm summers).

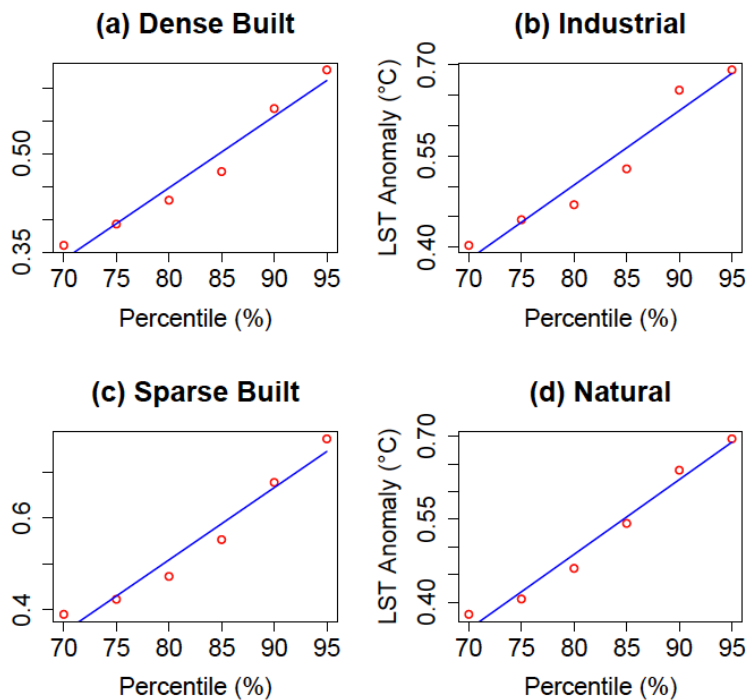


Figure 10. Regressions for LST-anomalies as a function of heat-wave percentile for each LCZ group (Cool summers).

Table 3a. Statistical summary for exponential regressions of LST-anomalies as a function of heat-wave percentile (a , b , R^2) and for comparison of various LCZ groups against a general relationship of all LCZ classes using a two-sample t-test (p -value) (Warm summers)

LCZ	a	b	R ²	p-value
Dense Built	-0.8126	0.03777	0.8158	0.6351
Industrial	-0.7407	0.03629	0.8835	0.8129
Sparse Built	-0.7396	0.04053	0.8888	0.9283
Natural	-0.6554	0.03468	0.8959	0.9414
All	-0.6892	0.03598	0.8847	NA

Table 3b. As per Table 3a, but for cool summers

LCZ	a	b	R ²	p-value
Dense Built	0.3396	0.0109	0.9612	0.5305
Industrial	0.3798	0.0122	0.9429	0.8387
Sparse Built	0.3513	0.01572	0.9564	0.7173
Natural	0.3515	0.0135	0.9757	0.9798
All	0.3502	0.01346	0.9727	NA

3.3. LCZ as a function of distance from downtown

Since the regressions for individual LCZ classes are not statistically significant with respect to increasingly extreme heat events, we then examined if LCZ as a function of distance from downtown is statistically significant. In order to find out whether knowing the LCZ class type can help us better predict the LST response, we examined the LST response by LCZ class as a function of distance from downtown. We consolidated the distance from downtown into 5 km bins. We looked at all summer days and all heat wave days. Outliers were removed using knowledge of the number of pixels by LCZ class in each 5 km bin (Table 4). We conducted a two-sample t-test to compare the difference in regression of individual LCZ classes and the general regression of all LCZ classes. The regressions are shown in shown in Figure 11 for all summer days and Figure 12 for all heat wave days. Table 5a and 5b show the statistical results of

the regressions for all summer days and all heat wave days respectively. The slope represents the change in LST ($^{\circ}\text{C}$) per km from downtown.

All the LCZ classes have a moderate to strong negative linear relationship with distance, with R^2 values between 0.6 and 0.8. The exception is LCZ A (trees), with a multiple R^2 value of 0.2655 for all summer days and 0.06894 for all heat wave days. This means that the linear regression of LST anomaly as a function of distance for LCZ A is weak. We also examined if the difference in regression between each LCZ class and all LCZ classes in general is statistically significant. The p-value for most LCZ classes is less than 0.05 (Table 5a and 5b), so the difference is statistically significant. The exceptions are LCZ 8 (large low rise) and LCZ B (scattered trees), whose p-values for all summer days are 0.542 and 0.2417 respectively. LCZ 10 (Heavy industry) have the steepest slope at $-0.08^{\circ}\text{C}/\text{km}$ whereas LCZ 9 (Sparsely built) have a slope of $-0.013^{\circ}\text{C}/\text{km}$ for all summer days and $-0.016^{\circ}\text{C}/\text{km}$ for all heat wave days. In other words, we know more information about the LST response as a function of distance when we know the LCZ class type for most LCZ classes, except for LCZ 8 and LCZ B.

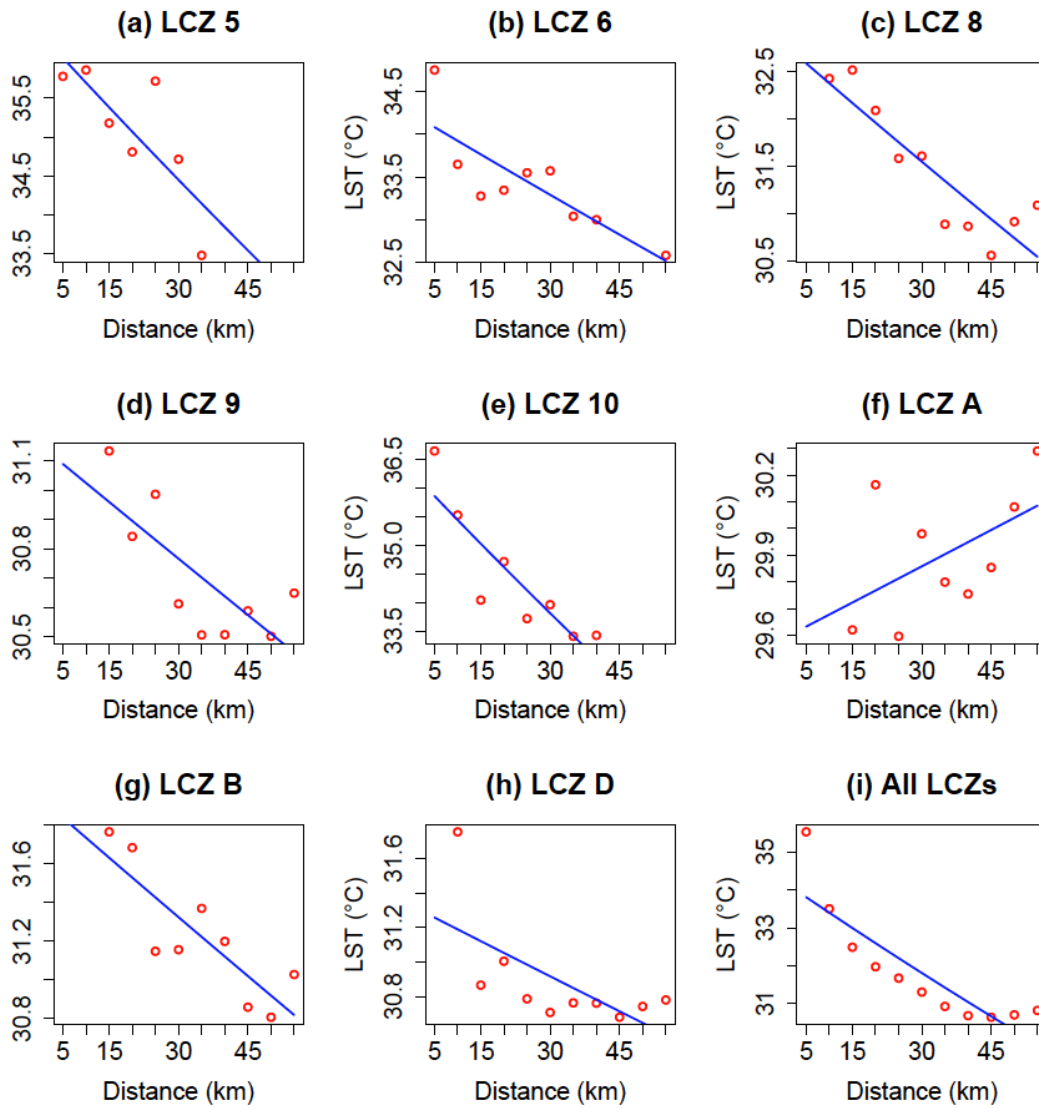


Figure 11. Regressions for LST-anomalies as a function of distance from city center for each LCZ class on all summer days. The red dots represent the median LST response for every 5th percentile and the blue line is the best-fit linear curve.

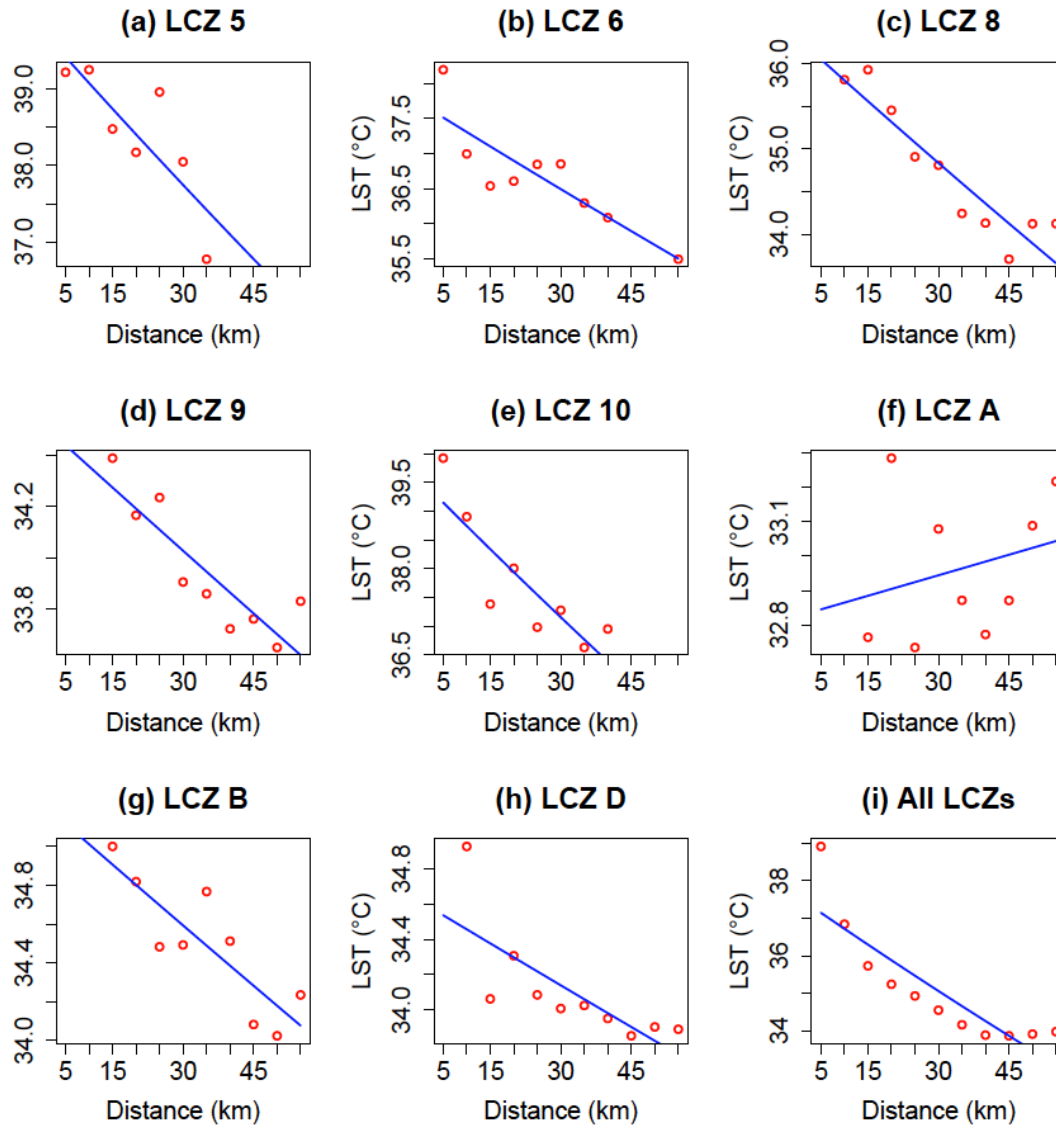


Figure 12. Regressions for LST as a function of distance from city center for each LCZ class on all heat wave days. The red dots represent the median LST response for every 5th percentile and the blue line is the best-fit linear curve.

Table 4. Number of pixels by LCZ class in each 5km bin

Distance (km)	LCZ 5	LCZ 6	LCZ 8	LCZ 9	LCZ 10	LCZ A	LCZ B	LCZ D	All LCZs
1-5	13	42	9	0	37	0	0	3	104
6-10	17	209	13	13	25	6	0	21	304
11-15	14	305	9	63	9	24	1	79	504
15-20	23	232	16	131	24	55	12	205	698
21-25	29	221	28	157	19	59	22	339	874

26-30	16	186	29	148	13	76	39	425	932
31-35	14	102	22	125	12	114	50	537	976
36-40	3	26	30	106	4	154	63	641	1027
41-45	1	5	50	95	0	205	71	706	1133
46-50	1	8	44	110	2	219	67	749	1200
51-55	1	21	89	82	3	198	69	682	1145

Table 5a. Statistical summary for linear regression of LST-anomalies as a function of distance (a , b , R^2) and for comparison of various LCZ classes against a general relationship of all LCZ classes using a two-sample t -test (p -value)
(All summer days)

LCZ	a	b	R ²	p-value
5	36.31519	-0.06192	0.6238	5.191e-05
6	34.242278	-0.031579	0.6785	0.004609
8	32.7844	-0.041	0.7836	0.542
9	31.1533	-0.01287	0.5822	0.02357
10	36.28	-0.08205	0.7706	0.002413
A	29.586	0.009074	0.2655	0.0005529
B	31.938	-0.0204	0.7064	0.2417
D	31.329	-0.01366	0.4209	0.0456
All	34.223	-0.07962	0.7493	NA

Table 5b. As per Table 5a, but for all heat wave days

LCZ	a	b	R ²	p-value
5	39.732	-0.0659	0.6749	7.316e-05
6	37.7133	-0.0405	0.7441	0.008287
8	36.2765	-0.0478	0.851	0.6014
9	34.5177	-0.0163	0.7701	0.02789
10	39.5556	-0.0799	0.7466	0.001813
A	32.8255	0.00398	0.06894	0.0003894
B	35.2168	-0.02076	0.7225	0.2621
D	34.617	-0.01586	0.5725	0.0445
All	37.5706	-0.08248	0.7556	NA

Now that we have confidence in the statistical significance of LST response by LCZ class as a function of distance from downtown, we can examine the spatial pattern of LST in more detail. To better understand the relationship between urban morphology and temperature

anomaly, we examined the spatial distribution of the LST response across downtown Kansas City for the most extreme heat events. The maps in Figure 13 excluded LCZ 8 and LCZ B, whose regressions as a function of distance from downtown are found to be not statistically significant (Table 5a and 5b). As such, the dense urban built-type classes shown on the maps are LCZ 5 and 6 (Figure 13a and 13d); sparse urban built-type/industrial classes are LCZ 9 and 10 (Figure 13b and 13e) and the natural land cover type classes are LCZ A and D (Figure 13c and 13f). We examined the spatial distribution of the LST anomaly response at the 75-80 percentile (Figure 13a to 13c) and at the 95-100 percentile (Figure 13d to 13f). We found that the higher heat anomalies can be found generally in the outlying areas in all LCZ groups, though the pattern is more pronounced in the 95th percentile cases (Figure 13d to 13f). These indicate that while the LCZ class regressions are not statistically significant with respect to increasingly extreme heat events, they are statistically significant as a function of distance from downtown. In other words, while knowledge of LCZ classes do not tell us more information about the LST response to more severe heat events, knowing the LCZ class is useful from the standpoint of where it is located with respect to the city center.

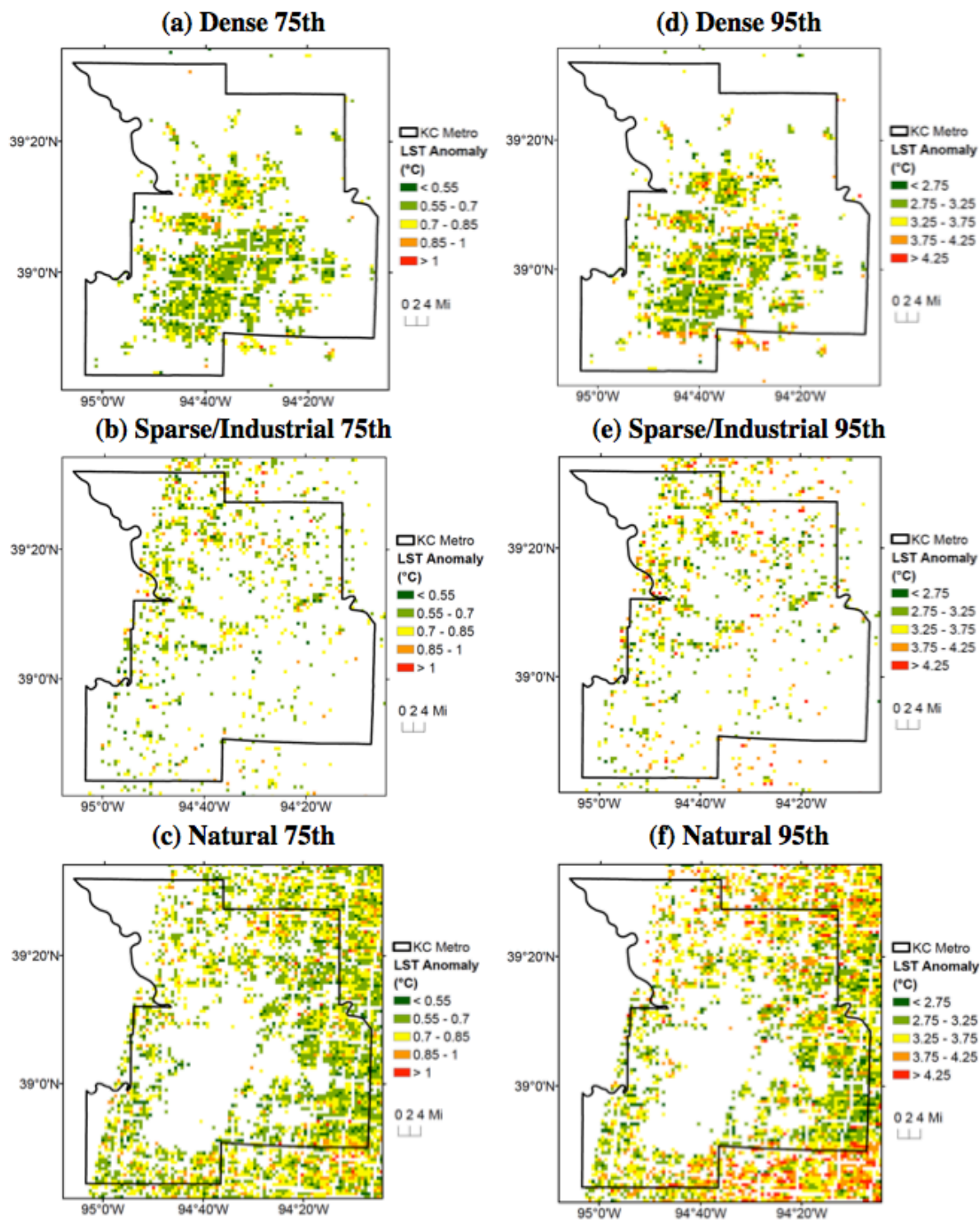


Figure 13. Spatial distribution of the LST anomalies at the 75-80 percentile level across the Kansas City metropolitan area for LCZ class (a) 5 and 6 (b) 9 and 10 & (c) A and D; At the 95-100 percentile level for LCZ class (d) 5 and 6 (e) 8 and 10 & (f) A and D.

CHAPTER 4

Discussion and conclusion

In this research, we used a LCZ classification scheme to represent morphology in the city center and surrounding areas (Figure 1a and Table 1). We hypothesized that the spatial pattern of UHI would be analogous to the spatial pattern of LCZs, i.e. that areas of most densely built environment correspond to areas of highest UHI. We used all available summer MODIS LST data from 2003 to 2017 to study the LST distribution by LCZ class during heat wave events, which we define to be from 70-100 percentile. Figure 3 shows that LST for all the LCZ classes warm with increasingly extreme heat events. But when we examined if different LCZ classes warm differently, the difference between regressions for individual LCZ classes and that of all LCZ classes is not statistically significant (Table 2). We then examined the LST response for all the years in our study period (Figure 5) and singled out 2004 and 2012 as the years with the lowest and highest LST anomalies respectively. 2004 and 2012 are also the coolest and hottest summers during our study period, with respect to the number of heat wave days. We examined the spatial distribution of mean LST (Figure 6) and LST anomalies (Figure 7) for the months of July and August in those two years. During the cool summer of 2004, the downtown area shows a higher LST anomaly than outlying areas (Figure 7a and 7b). However, during the warm summer of 2012, the pattern is reversed with outskirts showing a higher LST anomaly than the city center (Figure 7c and 7d). While the mean LST is warmer in the downtown area for both 2004 and 2012, there is also a zone of warmer LSTs in the outlying areas, especially to the southwest of downtown Kansas City in July and August 2012 (Figure 6c and 6d). This can possibly be explained by the higher LST anomalies in the outskirts during the extreme heat episodes in the anomalously hot summer.

We then decomposed all the years into the 7 warmest and 8 coolest summers (Figure 8) and tested the regressions of the four LCZ groups against increasingly extreme heat events (Figure 9 and 10). The regressions for the individual LCZ groups are found to be not statistically significant (Table 3a and 3b). Finally, we looked at the regressions of individual LCZ classes as a function of distance from urban core for all summer days (Figure 11) and all heat wave days (Figure 12). The regressions for most LCZ classes with the exception of LCZ 8 and LCZ B are found to be statistically significant (Table 5a and 5b). Of the six LCZ classes with statistically significant relationships, the slope ranges from $-0.08^{\circ}\text{C}/\text{km}$ to $-0.01^{\circ}\text{C}/\text{km}$. Therefore, while knowledge of LCZ classes does not give more information for predicting UHI response in extreme heat events, the knowledge is useful from the standpoint of where the LCZ is located with respect to the city center. This is further illustrated in Figure 13, where the higher LST anomalies can be found towards the outlying areas regardless of LCZ class. The pattern is even more pronounced at the 95th percentile of all heat events (Figure 13d to 13f).

A possible explanation for the highest LST anomalies to occur over outlying vegetated areas is the onset of drought conditions during the most extreme heat wave. It is well-known that vegetation along with pervious land cover have a cooling effect on the surrounding environment, thereby resulting in lower temperatures (Delet-Barreto et al. 2016; Jenerette et al. 2011; Imhoff et al. 2010). Furthermore, vegetation restores moisture availability in urban areas and reactivates the negative feedback on urban temperatures associated with evaporation (Li and Bou-Zeid 2013). However during prolonged heat waves, soils dry up and lose their moisture. Dried up soil heats up more easily, thus leading to increased LST (Hauser et al. 2016; Hirschi et al. 2011). The anomalously hot summer of 2012 was precipitated by an abnormally dry and warm spring, which saw much of the Southwest and Central Great Plains setting record warmest springs and

experiencing drought conditions (Cook et al. 2015; Hoerling et al. 2014). The extreme heat and drought conditions likely overcame even the effects of irrigation in the city (Rippey 2015). The enhanced spring evapotranspiration from earlier vegetation activity resulted in soil moisture depletion that likely increased summer heating (Wolf et al. 2016). The effect was relevant for Kansas City, which lies in the Central Great Plains, a region with significant land-atmosphere coupling during the summer (Koster et al. 2004). Given the initial cooler LST to begin with, the LST anomalies for outlying areas with more pervious land cover were unsurprisingly greater than over impervious surfaces. Therefore, while dense urban morphology with higher buildings generally mean higher LST and UHI response during summers with average temperatures, the extreme drought in 2012 summer brought about an even higher LST anomaly in areas with abundant natural land cover.

Overall, the key finding of this research is that knowledge of the LCZ class is not as important for predicting LST response as the distance from the city center. This is despite the usefulness of the LCZ system in classifying cities worldwide and helping us to better understand UHI beyond the traditional urban-rural distinction. This also poses the question of the effect of heat mitigation by having vegetation cover or a relative abundance of open spaces during the most extreme heat episodes. While urban planners generally encourage increasing the amount of green spaces in cities to mitigate UHI (Sharma et al. 2016; Li et al. 2014), vegetation may not provide the expected cooling effect in the most extreme heat wave events, particularly when drought conditions have developed, such as in 2012. In the city, however, this may not be true due to the ability to continue irrigation in cities as opposed to natural areas on the outskirts. But with climate change, there will likely be more extreme heat days and more prolonged heat waves. We have seen that as heat events worsen beyond a certain threshold, the pervious land

and vegetative cover lose their cooling effect. There may be significant societal and public health implications for people who live in areas with relative abundance of greenery if the heat anomaly is higher than in highly urbanized areas with lots of buildings and concrete. As such, the statistically significant relationship of various LCZ classes as a function of distance from the city center that we found provides a potentially significant insight when developing policies to adapt to more extreme summers in the near future.

REFERENCES

Bechtel, B., and C. Daneke, 2012: Classification of Local Climate Zones Based on Multiple Earth Observation Data. *IEEE Journal of Selected Topics in Applied Earth Observations and Remote Sensing*, 5(4), 1191-1202.

Bechtel, B., 2015: A New Global Climatology of Annual Land Surface Temperature. *Remote Sens.*, 7, 2850-2870, doi: 10.3390/rs70302850.

Bechtel, B., and et al., 2015: Mapping Local Climate Zones for a Worldwide Database of the Form and Function of Cities. *ISPRS International Journal of Geo-Information*, 4, 199-219.

Bechtel, B., and et al., 2017a: Beyond the Urban Mask: Local Climate Zones as a Generic Descriptor of Urban Areas – Potential and Recent Developments. Joint Urban Remote Sensing Event (JURSE), Dubai, 5-7 March, 2017.

Bechtel, B., and et al., 2017b: Quality of Crowdsourced Data on Urban Morphology - The Human Influence Experiment (HUMINEX). *Urban Science* 1(2), 15, doi:10.3390/urbansci1020015.

Bryant-Stephens, T., 2009: Asthma Disparities in Urban Environments. *American Academy of Allergy, Asthma and Immunology*, 123, 1199-1206, doi:10.1016/j.jaci.2009.04.030.

Chang, F. and J. Wallace, 1987: Meteorological Conditions during Heat Waves and Droughts in the United States Great Plains. *Monthly Weather Review*, 115, 1253-1269.

Ching, J. and et al., 2018: World Urban Database and Access Portal Tools (WUDAPT), an urban weather, climate and environmental modeling infrastructure for the Anthropocene. *Bulletin of the American Meteorological Society*.

Connors, J. and et al., 2013: Landscape configuration and urban heat island effects: assessing the relationship between landscape characteristics and land surface temperature in Phoenix, Arizona, *Landscape Ecol.*, 28, 271–283, doi: 10.1007/s10980-012-9833-1.

Conrad, O., and et al. 2015: System for Automated Geoscientific Analyses (SAGA) v. 2.1.4. *Geosci. Model Dev.*, 8(7), 1991–2007, doi:10.5194/gmd-8-1991-2015.

Cook, B. and et al., 2015: Unprecedented 21st century drought risk in the American Southwest and Central Plains, *Sci. Adv.*, 1, e1400082.

Data USA, 2017: Kansas City, MO-KS Metro Area. Accessed 24 March 2017. [Available online at: <https://datausa.io/profile/geo/kansas-city-mo-ks-metro-area/>]

Declet-Barreto, J. and et al., 2016: Effects of Urban Vegetation on Mitigating Exposure of Vulnerable Populations to Excessive Heat in Cleveland, Ohio. *Weather, Climate, and Society*, 8, 507-524, doi: 10.1175/WCAS-D-15-0026.s1.

Fischer, E. and C. Schar, 2010: Consistent geographical patterns of changes in high-impact European heatwaves. *Nature Geoscience*, 3, 398-403, doi:10.1038/ngeo866.

Fowler, D., 2013: Heat-Related Deaths After an Extreme Heat Event – Four States, 2012, and United States, 1999–2009, *Morbidity and Mortality Weekly Report*, 62(22), 433-455.

Forzieri, G. and et al., 2016: Multi-hazard assessment in Europe under climate change. *Climatic Change*, 137, 105-119.

Gal, T. and et al., 2015: Comparison of two different Local Climate Zone mapping methods. ICUC9 - 9th International Conference on Urban Climate jointly with 12th Symposium on the Urban Environment.

Graham, D., et al. 2016: The relationship between neighbourhood tree canopy cover and heat-related ambulance calls during extreme heat events in Toronto, Canada. *Urban Forestry & Urban Greening*, 20, 180-186, 10.1016/j.ufug.2016.08.005.

Harlan, S. and et al., 2006: Neighborhood Microclimates and Vulnerability to Heat Stress. *Social Science & Medicine*, 63, 2847-2863, doi: 10.1016/j.socscimed.2006.07.030.

Hauser, M., and et al., 2016: Role of soil moisture versus recent climate change for the 2010 heat wave in Russia, *Geophys. Res. Lett.*, 43, 2819-2826, doi:10.1002/2016GL068036.

Hirschi, M. and et al., 2011: Observational evidence for soil-moisture impact on hot extremes in southeastern Europe, *Nature Geoscience*, 4, 17-21, doi: 10.1038/NGEO1032.

Hoerling, M. and et al., 2014: Causes and Predictability of the 2012 Great Plains Drought, *Bull. Amer. Meteor. Soc.*, 95, 269–282, <https://doi.org/10.1175/BAMS-D-13-00055.1>.

Hu, L. and N. Brunsell, 2013: The impact of temporal aggregation of land surface temperature data for surface urban heat island (SUHI) monitoring. *Remote Sensing of Environment*, 134, 162-174.

Hu, L. and et al., 2014: How can we use MODIS land surface temperature to validate long-term urban model simulations? *Journal of Geophysical Research: Atmospheres*, 119, 3185-3201.

Hu, L. and N. Brunsell, 2015: A new perspective to assess the urban heat island through remotely sensed atmospheric profiles. *Remote Sensing of Environment*, 158, 393-406.

Imhoff, M. and et al. 2010: Remote sensing of the urban heat island effect across biomes in the continental USA. *Remote Sens. Environ.*, 114, 504-513, doi:10.1016/j.rse.2009.10.008.

Intergovernmental Panel on Climate Change (IPCC), 2014: Climate Change 2014: Synthesis Report. Contribution of Working Groups I, II and III to the Fifth Assessment Report of the Intergovernmental Panel on Climate Change [Core Writing Team, R.K. Pachauri and L.A.

Meyer (eds.)], Geneva, Switzerland, 151 pp.

Jang, K. and et al., 2014: Retrievals of All-Weather Daily Air Temperature Using MODIS and AMSR-E Data. *Remote Sens.*, 6, 8387-8404, doi: 10.3390/rs6098387.

Jenerette, G. and et al., 2016: Micro-scale urban surface temperatures are related to land-cover features and residential heat related health impacts in Phoenix, AZ USA, *Landscape Ecol*, 31, 745–760, DOI 10.1007/s10980-015-0284-3.

Koster, R. and et al., 2004: Regions of Strong Coupling Between Soil Moisture and Precipitation. *Science*, 305(5687), 1138-1140.

Kovats, R. and S. Hajat, 2007: Heat Stress and Public Health: A Critical Review. *Annual Review of Public Health*, 29, 41-55, 10.1146/annurev.publhealth.29.020907.090843.

Laaidi, K. and et al., 2012: The Impact of Heat Islands on Mortality in Paris during the August 2003 Heat Wave. *Environmental Health Perspectives*, 120(2), 254-259.

Lemordant, L. and et al., 2016: Modification of land-atmosphere interactions by CO2 effects: Implications for summer dryness and heat wave amplitude. *Geophysical Research Letters*, 43(19), 10240-10248.

Li, D. and E. Bou-Zeid, 2013: Synergistic Interactions between Urban Heat Islands and Heat

Waves: The Impact in Cities Is Larger than the Sum of Its Parts. *Journal of Applied Meteorology and Climatology*, 52, 2051-2064, doi: 10.1175/JAMC-D-13-02.1.

Li, D. and et al., 2014: The effectiveness of cool and green roofs as urban heat island mitigation strategies. *Environmental Research Letters*, 9, 055002.

Li, Z. and et al., 2013: Satellite-derived land surface temperature: Current status and perspectives. *Remote Sensing of Environment*, 131, 14–37, doi: 10.1016/j.rse.2012.12.008.

Loikith, P. and A. Broccoli, 2012: Characteristics of Observed Atmospheric Circulation Patterns Associated with Temperature Extremes over North America. *Journal of Climate*, 25, 7266-7281, doi: 10.1175/JCLI-D-11-00709.1.

McCarthy, M. and et al., 2010: Climate change in cities due to global warming and urban effects. *Geophys. Res. Lett.*, 37, L09705, doi:10.1029/2010GL042845.

Martin, P. and et al., 2015: An alternative method to characterize the surface urban heat island. *Int J Biometeorol*, 59(7), 849-861.

Meehl, G. and C. Tebaldi, 2004: More intense, more frequent, and longer lasting heat waves in the 21st century. *Science*, 305, 994–997, doi: 10.1126/science.1098704.

Monaghan, A. and et al., 2014: Evaluating the impact of urban morphology configurations on the accuracy of urban canopy model temperature simulations with MODIS. *J. Geophys. Res. Atmos.*, 119, 6376-6392, doi: 10.1002/2013JD021227.

Mutiibwa, D. and et al., 2015: Land Surface Temperature and Surface Air Temperature in Complex Terrain. *IEEE Journal of Selected Topics in Applied Earth and Remote Sensing*. 8(10), 4762-4774, doi: 10.1109/JSTARS.2015.2468594

NOAA National Centers for Environmental Information (NCEI), State of the Climate: Drought for June 2012, published online July 2012, retrieved on January 7, 2018 from <https://www.ncdc.noaa.gov/sotc/drought/201206>.

Oke, T., 1982: The energetic basis of the urban heat island. *Q J R Meteorol Soc.*, 108, 1-24.

Oke, T., 1988: Street design and urban canopy layer climate. *Energy and Buildings*, 11(1), 103-113, doi: 10.1016/0378-7788(88)90026-6.

Oke, T., 2006: Towards better communication in urban climate. *Theor. Appl. Climatol.*, 84, 179-190.

Oke, T., and et al., 2017: *Urban Climates*. Cambridge University Press, doi: 9781139016476.

Oleson, K. and et al., 2011: An examination of urban heat island characteristics in a global climate model. *Int. J. Climatol.* 31, 1848-1865, doi: 10.1002/joc.2201.

Peng, R. and et al., 2011: Toward a quantitative estimate of future heat wave mortality under global climate change. *Environ. Health Perspect.*, 119, 701–706, doi:10.1289/ehp.1002430.

Prihodko, L. and S. Goward, 1997: Estimation of air temperature from remotely sensed surface observations. *Remote Sensing of Environment*, 60(3), 335-346, doi: 10.1016/S0034-4257(96)00216-7.

Ramamurthy, P., and E. Bou-Zeid, 2017: Heatwaves and urban heat islands: A comparative analysis of multiple cities. *Journal of Geophysical Research: Atmospheres*, 122, 168-178.

Rippey, B., 2015: The U.S. drought of 2012, *Weather and Climate Extremes*, 10, 57–64, doi: 10.1016/j.wace.2015.10.004.

Robinson, P., 2000: On the Definition of a Heat Wave, *Journal of Applied Meteorology*, 40, 762-775.

Roth, M., 2013: Urban Heat Islands. *Handbook of Environmental Fluid Dynamics, Volume Two*. CRC Press/Taylor & Francis Group, LLC.

Russo, S. and et al., 2014: Magnitude of extreme heat waves in present climate and their projection in a warming world. *Journal of Geophysical Research: Atmospheres*, 119, 12500-12512.

Schatz, J. and C. Kucharik, 2015: Urban climate effects on extreme temperatures in Madison, Wisconsin, USA. *Environ. Res. Lett.*, 10, 094024, doi: 10.1088/1748-9326/10/9/094024.

Sharma, A. and et al., 2016: Green and cool roofs to mitigate urban heat island effects in the Chicago metropolitan area: evaluation with a regional climate model. *Environmental Research Letters*, 11, 064004.

Smargiassi, A., et al., 2009: Variation of daily warm season mortality as a function of micro-urban heat islands. *J Epidemiol Community Health*, 63:659–664, doi: 10.1136/jech.2008.078147.

Sohrabinia, M. and et al., 2015: Spatio-temporal analysis of the relationship between LST from MODIS and air temperature in New Zealand. *Theoretical and applied climatology*, 119(3), 567-583, doi: 10.1007/s00704-014-1106-2.

Stewart, I. and T. Oke, 2009: Classifying Urban Climate Field Sites By “Local Climate Zones”: The Case of Nagano, Japan. *The seventh International Conference on Urban Climate*.

Stewart, I. and T. Oke, 2012: *Local Climate Zones for Urban Temperature Studies*. American Meteorological Society, 1880-1900, DOI:10.1175/BAMS-D-11-00019.1

Tayyebi, A., and G. Jenerette, 2016: Increases in the climate change adaptation effectiveness and availability of vegetation across a coastal to desert climate gradient in metropolitan Los Angeles, CA, USA. *Science of the Total Environment*, 548, 60-71.

Tomlinson, C. and et al., 2011: Remote sensing land surface temperature for meteorology and climatology: a review. *Meteorol. Appl.*, 18, 296–306, doi: 10.1002/met.287.

Trenberth, K. and et al. 2015: How climate change affects extreme weather events. *Natural Climate Change*, 5, 725-730.

Unger, J., 2004: Intra-urban relationship between surface geometry and urban heat island: review and new approach. *Climate Research*, 27, 253-264.

University of Nebraska-Lincoln (UNL) National Drought Mitigation Center (NDMC), Central U.S. 2012 Drought Assessment, published online 2012, retrieved on January 7, 2018 from <http://drought.unl.edu/Portals/0/docs/CentralUSDroughtAssessment2012.pdf>.

Vardoulakis, S. and et al. 2003: Modelling air quality in street canyons – a review. *Atmospheric Environment*, 37, 155-182.

Voogt, J. and Oke, T. 2003: Thermal remote sensing of urban climates. *Remote Sensing of Environment*, 86(3), 370-384.

Wolf, S. and et al. 2016: Warm spring reduced carbon cycle impact of the 2012 US summer drought, PNAS, 113(21), 5880-5885.

Wood, C. and et al., 2013: An Overview of the Urban Boundary Layer Atmosphere Network in Helsinki, Bulletin of the American Meteorological Society, 94(11), 1676-1690.

World Health Organization (WHO), Center for Health Development, United Nations Human Settlements Programme. 2010: Hidden Cities: Unmasking and overcoming health inequities in urban settings.

Yang, Y. and et al., 2017: Evaluation of MODIS Land Surface Temperature Data to Estimate Near-Surface Air Temperature in Northeast China. Remote Sens., 9, 410, doi:10.3390/rs9050410.

Zeng, L. and et al., 2015: Estimation of Daily Air Temperature Based on MODIS Land Surface Temperature Products over the Corn Belt in the US. Remote Sens., 7(1), 951-970; doi:10.3390/rs70100951.

Zhang, J. and et al., 2015: Retrieval of the land surface-air temperature difference from high spatial resolution satellite observations over complex surfaces in the Tibetan Plateau. J. Geophys. Res. Atmos., 120, 8065–8079, doi:10.1002/2015JD023395.

Zhao, L. and et al., 2017: Interactions between urban heat islands and heat waves, *Environmental Research Letters*, in press.

Zhou, B. and et al., 2017: The role of city size and urban form in the surface urban heat island, *Nature*, 7, 479, doi: 10.1038/s41598-017-04242-2.

Zhou, X. and Y. Wang, 2011: Dynamics of Land Surface Temperature in Response to Land-Use/Cover Change, *Geographical Research*, 49: 23–36, doi:10.1111/j.1745-5871.2010.00686.x.